MATERIAL PROPERTIES AND MODELS FOR THE ASSESSMENT OF PRESSURE BARRIER FAILURE IN HIGH-PRESSURE CORE MELT ACCIDENT SCENARIOS

Christoph Bläsius[1], Annett Udoh[2], Jürgen Sievers[3]

[1] Technical Expert Structural Mechanics, GRS gGmbH, Cologne, Germany (christoph.blaesius@grs.de)
[2] Research Scientist, Materials Testing Institute, University of Stuttgart, Stuttgart, Germany
[3] Chief Expert Structural Mechanics, GRS gGmbH, Cologne, Germany

ABSTRACT

The paper addresses the process of acquiring material data and setting up reliable material models for the assessment of pressure barrier mechanical failure in the extreme loading regime of high-pressure core melt accidents, considering typical steels used in Western Light Water Reactors with a focus on German steel grades. Prominent issues include the consideration of particular deformation, damage, and failure mechanisms, a literature survey on available data, ways to overcome a lack of data, including additional experimental work on short-term-creep of Alloy 800 (mod.), and a discussion about the limits of accuracy.

INTRODUCTION

During postulated high-pressure core melt accident scenarios, components of the reactor pressure barrier, such as piping, flanges, penetrations and valves, can experience extreme loading from inner pressure and hot gases from the core melt process, even before a substantial amount of melt is relocated to the RPV lower plenum. Time, mode and location of resulting leaks or ruptures with subsequent partial or full reactor depressurization can have crucial effects on the further course of the accident and the distribution of hydrogen and radionuclides. A particular threat arises from failure locations that can induce a containment bypass, such as High-Pressure Melt Ejection and Direct Containment Heating (HPME/DCH), Consequential Steam Generator Tube Rupture (C-SGTR), leakage through specific instrumentations or secondary containment damage due to sudden energy release.

Mechanical failure assessments of pressure barrier critical components using simple or sophisticated methods, such as Finite Element (FE) modelling, require suitable material data and models. The material behavior in this particular loading regime poses specific challenges. As it is far beyond the usual range of application, experimental studies are rare. Furthermore, it poses its own peculiarities and phenomena that have to be considered.

MATERIAL BEHAVIOR

Relevant pressure barrier materials

The pressure barrier of Western Light Water Reactors is made from various steel grades depending on country, manufacturer and time of construction. For the purpose of high-temperature failure analysis, these can be coarsely categorized into three main classes that show largely similar thermal and mechanical properties. The first group comprises ferritic low alloy steels that are used for the manufacturing of the RPV and, particularly in German KWU-type reactors, the large piping of the Reactor Cooling System (RCS) and

the corpus of the steam generator. Typical representatives are the German grade 20 MnMoNi 5 5 and the similar grades SA 533B1 and 16 MND 5. After forging/rolling, quenching and tempering they show a good combination of strength and ductility at operational temperatures. The second group comprises austenitic high alloy steels, such as the German grades X 10 CrNiNb 18 9/X6 CrNiNb 18 10 S and the steels SS304 or SS316 that are used also for piping and nozzles as well as for cladding of ferritic components. They possess good corrosion resistance and high ductility. The strength properties are lower compared to ferritic steels at operational temperature but decline more slowly with temperature. A third group comprises nickel-based or nickel-rich alloys used mainly for steam generator tubes, such as the German grade Alloy 800 (mod.) and the steels Alloy 690 and Alloy 600. They are essentially austenitic high alloy steels with an increased nickel content.

Beside these three main groups, other materials can be found in niches. High-strength ferritic or martensitic steels are used for bolts. Welding materials typically overmatch the surrounding material at operational temperature. The thick pump housings are made of cast steel. Sealings are made of different materials, such as austenitic steel or graphite on perforated steel sheets. In the considered failure assessment, the representation of these special materials may be simplified or reduced to those properties that are expected to have an influence on the analysis results. In the following, these will not be further considered.

Deformation, damage and failure mechanisms

The behavior of steels in the loading regime shows some particularities. The most prominent one is that at high temperatures, beside elastic and plastic deformation, creep deformation has to be taken into account. Creep describes a time-dependent deformation, that arises already below yield strength and can be divided into degressive primary, constant secondary and progressive tertiary creep stage (Figure 1, left). From experience, creep can be described by the Norton-Bailey/Arrhenius equation (Rösler, Harders, & Bäker, 2012) (Equation 1), where $\dot{\varepsilon}_{cr}$ is creep strain rate, σ stress, T temperature, R universal gas constant, K, n, E_a, C constants.

$$\dot{\varepsilon}_{cr}(\sigma, T) = K * \sigma^n * e^{\frac{-E_a * C}{RT}} \tag{1}$$

Most of creep assessment in literature is dedicated to long-term creep and lifetime analysis, e.g. for turbine blades, while relevant events in a high-pressure core melt accident happen within a much shorter timeframe. Creep is an umbrella term for several time-dependent deformation mechanisms and the here relevant short-term deformation can be largely attributed to dislocation creep (Figure 1, middle) (Abd El-Azim, 1996). Dislocation creep shows phenomenological similarities with plasticity (dislocation slide) and a strict distinction on microstructural level is difficult (Ringel & Stelling, 2005). Theoretical models for dislocation creep predicted a stress exponent of n = 3 (Rösler, Harders, & Bäker, 2012). According to theory, steels show none or little primary creep in the loading range (Webster & Ainsworth, 1994), which corresponds well with observations (Thinnes, et al., 1994), (Schemmel & Schellenberg, 1999).

Correlations between creep and tensile data were subject to a variety of investigations (Abd El-Azim, 1996). For dislocation creep, it was found that tensile data essentially follows equation 1 with the same coefficients as for creep, when instead of $\dot{\varepsilon}_{cr}$ the externally applied strain rate, and for σ the saturation stress is inserted. The correlation was validated for Alloy 800H at 850 °C (Abd El-Azim, 1996), for stainless steels SS316, SUS316(N), CF8M and for carbon steel STS410 (Harada, et al., 2000), (Harada, et al., 2012).

A specific behavior of the group of ferritic steels is the ferrite-to-austenite phase transformation during heat-up at temperatures around 1000 K that can alter material properties, especially thermal and strength properties, considerably (Thinnes, et al., 1994). In the transformation interval, the material represents a compound of two phases and the material properties are determined by the relative volume

fractions (Humphries, 2002). The differences in density between the constituents can induce transformation stresses, but these are of second order (Humphries, 2002).

Giving the classification of (Ashby & Dyson, 1984), seven damage and failure mechanisms are relevant for the considered steels in the specific loading regime: macroscopic geometry change and necking, ductile fracture after transgranular damage, creep failure after intergranular damage, changes and peculiarities of microscopic structure, surface corrosion and complex failure modes on component level.

Macroscopic geometry changes are particularly relevant as elongation at fracture and reduction of area are often high and increase further with temperature (Ringel & Stelling, 2005). Elongation inevitably leads to a thinning of the specimen or component wall and subsequently a stress-increase, building a self-reinforcing process. In piping and vessels, this process can be further reinforced by a load increase due to bloating. Above the temperature-dependent yield stress, creep strain can be accompanied by plastic strain. When no other failure mechanism interferes, failure under primary loads is caused by plastic instability (Swift, 1952) or creep necking (Burke & Nix, 1975). Under secondary loads and without internal damage, there would be a failure surface without pores and perfect tips. Several investigations indicate that for the relevant materials, macroscopic geometry changes rather than internal metallurgy are the essential origin of tertiary creep in load-controlled tests (Thinnes, et al., 1994), (Eisert, Bachmann, & Sievers, 2003), which was proven by comparison to stress-controlled tests.

Only at comparably higher strains, when plastic instability may be already exceeded, a certain influence of internal damage was found (Willschütz, 2005). This damage is mostly of transgranular type with phenomenology similar to ductile damage (Figure 1, right). Metallographic examinations found the same honeycomb structure as in the hot tensile tests (Ringel & Stelling, 2005). The elongations at fracture were comparable with those from hot tensile tests and mostly independent from stress. At low stresses and long times compared to the relevant loading regime, also intergranular creep damage and fracture has been found, leading to reduced failure strains (Ringel & Stelling, 2005).
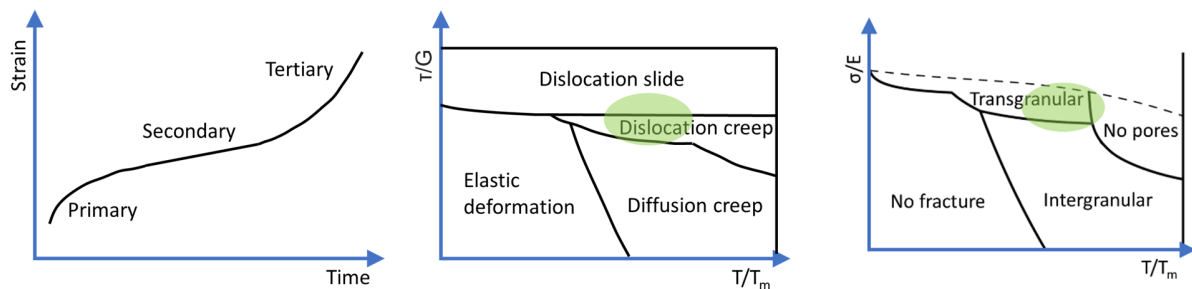
Figure 1. Schematic representation of creep deformation (left), deformation and failure mode map according to (Rösler, Harders, & Bäker, 2012) with loading regime (green), shear stress τ, shear modulus G, normal stress σ, Young's modulus E, absolute temperature T, melt temperature T_m (middle/right)

A further group encompasses a row of microstructural damage and failure mechanisms specific to particular steels, essentially reducing failure strain. The most prominent one goes back to the observed different failure behavior of ferritic steel SA533B1 in the sequential research programs LHF and OLHF (Humphries, 2002). While in the LHF experiments intergranular fracture with low failure strains and little necking was found, the material showed high ductility and pronounced necking in the OLHF experiments. It was later found that a 10 fold higher sulfur content, still within the steel specifications, was responsible for the intergranular fracture behavior. Steel X10 CrNiNb 18 9 showed a chromium depletion of the grain

boundaries, which is associated with hot cracking (Weber & Schick, 1999). Alloy 800H is exposed to intergranular carbide precipitation in the temperature range 800-900 °C (Abd El-Azim, 1996).

Surface oxidation has been observed especially at temperatures above 800 °C and long times (Obst & Maile, 1989). It is the reason for performing laboratory tests under protective gas atmosphere or vacuum (Thinnes, et al., 1994). Specific investigations on this issue showed that at least for ferritic steel 20 MnMoNi 5 5, mechanical properties of test specimens are only marginally influenced in times < 50 h (Obst & Maile, 1989).

Complex failure modes on component level can encompass instabilities, such as kinking, buckling or collapse (Kasahara, et al., 2015), excessive deformations without non-linearity or component-specific failures, like the building of a flange leak or the jamming of a valve.

ACQUISITION OF TEST DATA

Literature survey on available data

As previously mentioned, test data in the specific loading regime is rare. Most of the data stems from investigations in the frame of RPV failure investigations, which tendentially encompasses lower stresses and higher temperatures. A literature survey was performed predominantly for German steels 20 MnMoNi 5 5, X 10 CrNiNb 18 9/X6 CrNiNb 18 10 S and Alloy 800 (mod.), but also for similar foreign grades SA 533B1, 16 MND 5, SS304, SS316, Alloy 690 and Alloy 600 to enrich the available data base. The set of properties aimed to collect was grouped into general data, thermophysical properties, elastic/plastic properties, short-term creep properties, fracture behavior and derived model and engineering coefficients. The sources included data sheets, journal or conference papers, reports or text embedded in documents written on a different topic, e. g. numerical simulation. The collection was aided by a spreadsheet matrix, where the availability of the material properties in the literature sources was summarized.

Over 200 publications were evaluated, whose full presentation and comparison would go beyond the scope of this paper. Particularly important contributions and overviews for low alloy ferritic steels can be found in, (Obst & Maile, 1989), (Schemmel & Schellenberg, 1999), (Ringel & Stelling, 2005), (Krompholz & Kalkhof, 2002) for 20 MnMoNi 5 5, (Rempe, et al., 1993), (Daw, Rempe, & Knudson, 2009), (Humphries, 2002), (Yamaguchi, 2020) for SA 533B1, (Willschütz & Altstadt, 2002), (Sainte Catherine, 1998) for 16MND5. Data for high alloy austenitic steels can be found among others in (Bathe, Maile, & Obst, 1991), (Weber & Schick, 1999) for X 10 CrNiNb 18 9/X6 CrNiNb 18 10 S, (Rempe, et al., 1993), (Kato, Hasebe, & Yoshida, 2008), (Daw, Rempe, & Knudson, 2009), (Shimomura, et al., 2017), (Onizawa & Wakai, 2019) for SS304, (Harada, et al., 2000), (Kato, Hasebe, & Yoshida, 2008), (Harada, et al., 2012), (Shimomura, et al., 2017), (Onizawa & Wakai, 2019), for SS316. Data for nickel-based/high-nickel alloys is included for example in (Rempe, et al., 1993), (Chavez, et al., 1994), (Daw, Rempe, & Knudson, 2009), (Yamaguchi, 2020) for Alloy 600. The available material data base covers a broad part of the loading regime, except for Alloy 800 (mod.), for which no reference was available for short-term creep behavior.

Short-term creep of Alloy 800 (mod.)

To address the deficiency in short-term creep data of nickel-based/nickel-rich alloys, in particular Alloy 800 (mod.), a test series was performed at the Materials Testing Institute of the University of Stuttgart. The tests were performed on flat specimens prepared from an original workpiece of a steam generator tube (Figure 2, left). The preparation procedure was already qualified in a previous project (Gehrlicher & Seidenfuß, 2013). Strain was measured using an extensometer and via machine path. The temperature was applied via a furnace controlled by a thermocouple. In the first specimens, it came to a

failure in the fixation, which limited the maximally measured strain but had no further effect on results. In later specimens, it was addressed by additional reinforcements welded to the fixation (Figure 2, left).

To reduce time, costs and need for original material, instead of a comprehensive material characterization, an optimized testing procedure was applied (Figure 2, right). At first, two heat-up tests (V1, V2) were performed at constant loads (Figure 3, left). These loads were derived from the application scenario: In the typical accident, pressure of the primary side (inside the tubes) is defined by the safety valve opening pressure while the secondary side (outside the tubes) is either at nominal or zero pressure. Together with a typical tube geometry and after conversion to a uniaxial value, loads were obtained. The aim of the heat-up tests was primarily to identify the parameter space for the subsequent creep tests. Furthermore, it should be verified that the material behaves ductile in the relevant parameter space. The heat-up rate was determined as average from several thermohydraulic calculations for accident analyses, which, as an additional result, delivers temperature values that can be used as a rough estimation for damage and failure when no better model is available. Deviations from purely thermal expansion were observed at 810 and 854 °C, respectively. A strain value of 5 % was reached at 880 and 920 °C.
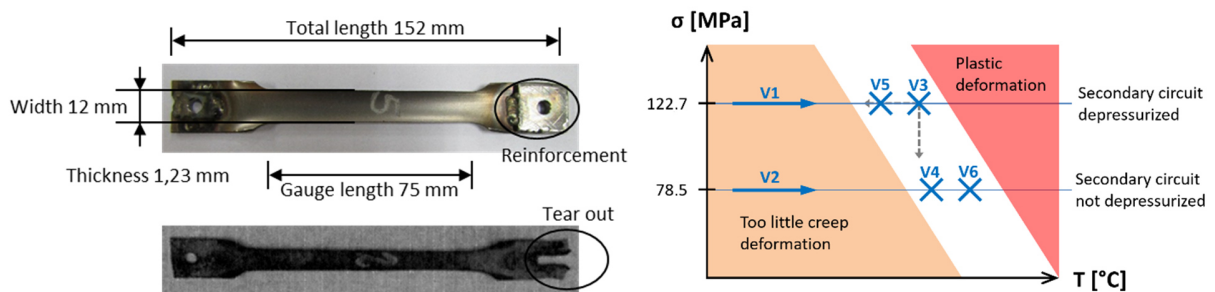
Figure 2. Test specimens before and after testing (left), schematic representation of the experimental boundary conditions in the parameter space (right)

In a next step, four short-term creep tests were performed within the identified parameter range, using temperatures of 810 and 854 °C, respectively (Figure 3, right). As only three tests are necessary to span the stress and temperature dimension, the fourth acted as a reserve, which had to be used when specimen 4 showed a creep strain rate outside the relevant parameter space. Fracture occurred beyond a total strain of 30 % and was not exactly measured. Negligible primary creep was observed and tertiary creep could be attributed to macroscopic geometry changes as later proven by 3D FE recalculations.
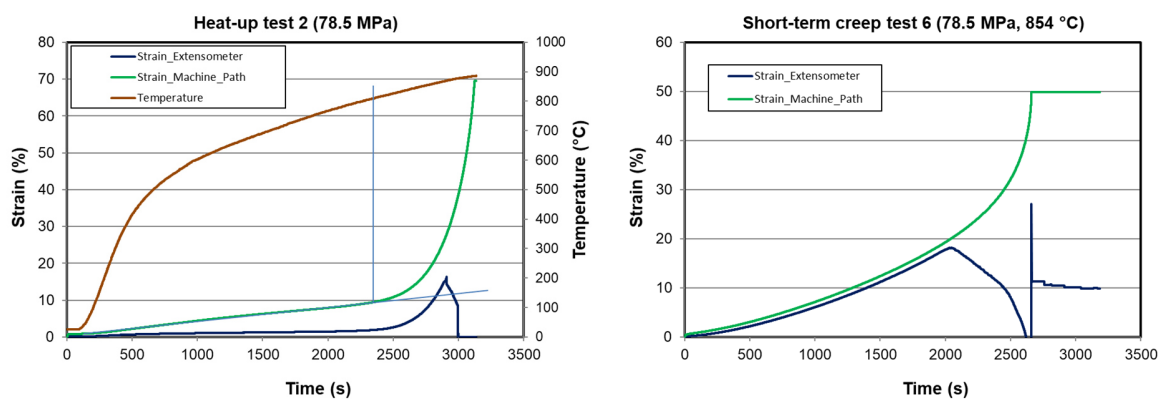
Figure 3. Example of a heat-up test (left) and a short-term creep test (right)

Secondary strain rate was extracted from the experiments using a graphical approach. A combined Norton-Bailey/Arrhenius model (Equation 1) was fitted, leading to a first set of parameters (Table 1). To get more out of the data, the tests of all three chosen specimens together with the two initial heat-up tests were recalculated using a 3D FE model, adapting the parameters in an iterative manner using a macro until a minimum residuum was reached (Table 1). The low residuum tentatively indicated a moderate scatter between the tests. The coefficients are in agreement with theory (n = 3 for dislocation creep) and the experience with other steels in this range.

Table 1: Derived coefficients of equation 1 for Alloy 800 (mod.)

	K	$\frac{-E_a * C}{R}$	n
Reconstruction on specimens 3, 5, 6	15992.06	-38088.11	3.098
Iterative fitting macro on specimens 1, 2, 3, 5, 6	15049.04	-36154.47	2.8007

MODELLING PROCESS

Discussion of errors, scatter and uncertainties

In the here considered area of application, the predominant sources of scatter in material properties (provided macroscopic faultlessness and accordance to specifications) are variations in chemical composition, heat treatment and mechanical history (Chu, et al., 2002). Even seemingly insignificant variations can make a great, sometimes qualitative difference (Pilch, et al., 1998). Reactor steels that undergo a ferritic to austenitic phase transformation may show larger scatter in the transformation interval due to different proportions of transformed volume or dynamic recrystallization (Schemmel & Schellenberg, 1999). Above transition, the influence of the heat treatment decreases (Willschütz H. , 2005), so that scatter bands for strength values from hot tensile and creep tests are rather narrow (Obst & Maile, 1989) (Schemmel & Schellenberg, 1999).

A further source of scatter arises from inadequacies in the experimental setup in the laboratory. For example, it can be difficult to keep the temperature exact, while it is influenced by different processes including deformation itself, and creep scales disproportionally with temperature (Onizawa & Wakai, 2019; Onizawa & Wakai, 2019). In stress-controlled tests there could be an error in the readjustment due to time-lag or the transducer not measuring at the thinnest location, especially during necking (Obst & Maile, 1989). The previously discussed effects can at least partly explain the observed scatter. But even in the same batch and the same laboratory replica tests show a residual scatter (Pilch, et al., 1998), (Ringel & Stelling, 2005). It can reach values of up to ±30% for yield stress (Pilch, et al., 1998), (Willschütz, 2005) and -48%/+68% for short-term creep (Humphries, 2002).

A next source of uncertainty and scatter is connected to the transfer from test specimen to component and can be partly assessed using size effect studies. For ductile steels the influence of geometrical size is usually assumed to be negligible, provided the material is sound and not subject to corrosion or decarburization effects (ASTM, 2018). Nevertheless, heat treatment is less effective for thick components as thermal inertia reduces the maximum temperature transient with distance from surface, leading to an inhomogeneous property distribution (Azodi, et al., 1996). A statistical distribution of cavities and material properties has less influence on thick components due to averaging and supporting effects of the surrounding material (Willschütz, 2005), (Krompholz & Kalkhof, 2002). Especially for lower stress levels and longer test time, size influences due to the fact that diffusion does not scale with size may arise (Krompholz & Kalkhof, 2002). While tests are performed under vacuum or protective atmosphere, the surface of real components can interact with the surrounding air or corium and gasses from the core melt.

A last source of error arises from the transformation of raw data into material models, e.g. fitting errors or the neglection of secondary influences, such as load application velocity (Ringel & Stelling, 2005). Furthermore, the selection of raw data, the resolution and the parameter space have an influence on the accuracy of the material model. A model fitted to the parameter band of the specific use case or giving it more weight might be more exact than a model covering a broader band of applications and including qualitatively different phenomena. It makes a difference whether a material model is used for the recalculation of a specific experiment with given material data, or for the use in accident analysis in general (Humphries, 2002). Lastly, there can be modeler/user errors in the implementation and use of the material model that have to be prohibited by a careful implementation, verification/validation and description.

Implementation of the material model

For the implementation of the material model, the approach has to be chosen between traditional models, where total strain ε_{tot} is described as an arbitrary superposition of elastic ε_{el}, plastic ε_{pl} and creep strain ε_{cr} and more advanced types such as constitutive or damage mechanic models that take processes on microstructural level into account. In light of the largely ductile behavior with late internal damage, a relevant scatter (see next subsection) and the mostly monotonically increasing thermal and mechanical load in the use case, a traditional model is considered sufficient here.

While stress dependency of the elastic strain is described by Hooke's law, stress dependency of plastic strain can be described by simple approaches, such as bilinear or Ramberg-Osgood, or – as chosen here – by multilinear curves that are defined by a sufficient number of support points. The temperature dependency of the elastic and plastic stress is realized by different parameter sets for each temperature step. Technical stress-strain-curves have to be converted to true ones, as strains can become large (Equation 2). If stress-strain curves were generated using load-controlled tests, which are not able to obtain data beyond necking, extrapolation (constant, linear or analogue to similar steel) may become necessary.

$$\varepsilon_{true} = ln(1 + \varepsilon); \; \sigma_{true} = \sigma(1 + \varepsilon) \tag{2}$$

For the mathematical representation of creep strain or creep strain rate, numerous descriptions exist that take primary, secondary and/or tertiary creep into account. As primary creep has been shown low in the relevant loading regime for the relevant steels and tertiary creep could be largely contributed to macroscopic deformation, a description of secondary creep was considered sufficient, provided an updated lagrangian formulation is used for FE calculations. Although a Norton-Bailey/Arrhenius formulation (Equation 1) is closer to theory, a hyperbolic sine law (Equation 3) was chosen here, which is known to better describe creep behavior over a wide stress range. Fitting is performed on the extracted secondary creep rates using a scaled least square-fit, while keeping the coefficients within a certain range to avoid numerical issues. The temperature dependence is taken into account by the Arrhenius-term or alternatively by implementing different parameter sets for defined temperatures. An often-used alternative to the use of a formula is the implementation of a stress/temperature matrix, in which creep strain rate is nonlinearly interpolated at runtime, as in (Willschütz & Altstadt, 2002). The advantage is that a wider load range can be taken into account while the disadvantage is a missing smoothing of the data, especially when there is only one measurement available for every point of the matrix. It is therefore not considered here.

$$\dot{\varepsilon}_{cr}(\sigma) = C_1[sinh(C_2\sigma)]^{C_3} * e^{\frac{-E_a * C}{RT}} \tag{3}$$

Due to the scarcity of data in the considered parameter space and the efforts needed for its generation, it may become necessary to fill gaps by inter-/extrapolation and reconstruction, e.g. by using the generated correlations outside its experimental basis or using engineering parameters that go back to

the same equations, e.g. the Larson-Miller Parameter (Larson & Miller, 1952). A major problem then poses the existence of qualitative changes along the extrapolation dimension, such as change of deformation mechanism, damage/fracture mechanism, phase/microstructural changes or other effects, such as power-law breakdown. Stress exponent n and activation energy E_a tend to show higher values for short-term creep than for long-term creep (Maruyama, 2008). An advanced extrapolation method to address this problem was developed by (Wilshire & Battenbough, 2007) (see Whittaker, & Harrison, 2014). Another problem is that fitting errors will multiply with the range of extrapolation. Extrapolation curves may even overlap in sufficient distance. Aside purely numerical means, the correlation to similar materials or the proof of the extrapolation by conducting single specimen tests might then be an option.

The use of traditional material models makes a failure criterion necessary. The often largely ductile behavior with late transgranular damage suggests the use of conventional criteria for ductile failure that typically depend on triaxiality of the stress tensor, as given in (Rice & Tracey, 1969) or (Bao & Wierzbicki, 2004). True failure strains can be calculated from elongation at fracture using Bridgman formulas or more advanced approaches (Alves & Jones, 1997). Criteria specifically proposed for component integrity under severe accident loading are given in (Chavez, et al., 1995) and (Willschütz, 2005). When the combination of material and loading is prone to intergranular damage, further criteria or a generally conservative strain limit may become necessary. In practice, under primary loads plastic instability will be often reached before internal fracture, determined by Considére's criterion (Rösler, Harders, & Bäker, 2012) or, in case of FE calculations with updated lagrangian formulation, by numerical instability after an infinite rise in strain.

Of great importance is the verification and validation of the material model. This was done by comparing coefficients with theory and experience of other material models, testing of interpolation behavior, comparison with hand calculations and recalculation of experiments of small-scale specimens. Typical pitfalls may comprise confusion between secant and tangent coefficient of thermal expansion, confusion about units in numerical value equations, double consideration of tertiary creep in the material model and in the updated lagrangian formulation as well as unexpected interpolation behavior. The latter can be observed in some codes that perform linear interpolation between coefficients, which are subsequently inserted to the equation, instead of interpolation between equation results at defined base points, leading to unphysical values. Remedy can be the choice of a formulation less prone to this behavior, keeping the coefficients within a range or the insertion of additional (virtual) base points.

CONCLUSION

The paper presents the particularities and difficulties in acquiring material data and setting up material models for the assessment of pressure barrier mechanical failure in the loading regime of high-pressure core melt accidents. The first part discusses fundamental aspects. Relevant steels can be categorized into three main classes. In the loading regime, time-dependent dislocation creep has similarities with tensile deformation. Primary creep has been shown low and tertiary creep could be largely attributed to macroscopic deformation. Transgranular damage was usually observed at large strains. Intergranular fracture was only observed for low stresses, large times or for specific steel grades and temperatures.

The second part of the paper addressed the acquisition of test data. A short survey on available test data in literature is given. The majority of the data has been generated for integrity assessment of the RPV under severe accident loading, tendentially involving lower stresses and higher temperatures. Additional short-term creep tests were conducted using original material of Alloy 800 (mod.). In order to obtain reliable data at manageable efforts, an optimized testing procedure was applied.

In the third part of the paper, the actual transfer of material properties to material models was discussed. Uncertainties stemming from material production, testing, transferability from specimen to component and representation in the material model were summarized. Considerations for the choice of the

underlying material model type and the mathematical representations are discussed including limits for data extrapolation. The importance of verification/validation to avoid pitfalls is emphasized.

ACKNOWLEDGEMENTS

REFERENCES

Abd El-Azim, M. (1996). "Correlation Between Tensile and Creep Data in Alloy 800 H at 850 °C", *2nd International Conference on Heat Exchangers, Boilers & Pressure Vessels*, Alexandria, Egypt.

Alves, M., Jones, N. (1997). "Influence of hydrostatic stress on failure of axisymmetric notched specimens", *Journal of the Mechanics and Physics of Solids*, Vol. 47, pp. 643-667.

ASTM, American Society for Testing and Materials (2018). *ASTM E139-11(2018) Standard Test Methods for Conducting Creep, Creep-Rupture, and Stress-Rupture Tests of Metallic Materials*.

Ashby, M., Dyson, B. (1984). "Creep Damage Mechanics and Micromechanisms", *6th International Conference on Fracture ICF6*, New Delhi, India.

Azodi, D., Eisert, P., Gruner, P., Jendrich, U., Kuntze, W. (1996). *Verifizierung und internationaler Vergleich von Strukturanalysemethoden zur Beschreibung des Verhaltens des Reaktordruckbehälters bei Belastungen jenseits der Auslegungsgrenzen*, GRS mbH, GRS-A-2338. (in German)

Bao, Y., Wierzbicki, T. (2004). "A comparative study on various ductile crack formation criteria", *ASME Journal of Material Engineering Technology*, Vol. 126, pp. 314-324.

Bathe, K., Maile, K., Obst, V. (1991). *Untersuchungen der Materialeigenschaften unter auslegungsüberschreitenden Bedingungen*, MPA Stuttgart, Abschlussbericht 1500806 (in German)

Burke, M.A., Nix, W.D. (1975). "Plastic instabilities in tension creep", *Acta Metall.*, Vol. 23, pp. 793.

Chavez, S., Kelly, D., Witt, R., Stirn, D. (1995). "Comparison of stress-based and strain-based creep failure criteria for severe accident analysis", *Nuclear Engineering and Design*, Vol. 155, pp. 603-622.

Chavez, S., Korth, G., Harper, D., Walker, T. (1994). "High-temperature tensile and creep data for Inconel 600, 304 stainless steel and SA106B carbon steel", *Nuclear Eng. and Design*, Vol. 148, pp. 351-363.

Chu, T., Humphries, L., Lu, W., Mongabure, P., Robino, C. (2002). "Material Characterization in Support of OLHF Experiments", *OLHF Seminar*, Madrid, Spain.

Daw, J., Rempe, J., Knudson, D. (2009). *Thermal Properties of Structural Materials Found in Light Water Reactor Vessels*, Idaho National Laboratory, INL/EXT-09-16121.

Eisert, P., Bachmann, P., Sievers, J. (2003). *Weiterentwicklung der strukturmechanischen Analysemethodik zur Bestimmung des Kriechverhaltens von Komponenten*. GRS mbH, GRS-A-3104 (in German)

Gehrlicher, S., Seidenfuß, M. (2013). *Schädigungsmechanische Modellierung des Resttragvermögens von geschädigten Dampferzeugerheizrohren*, MPA Stuttgart, Abschlussbericht 3610R01385 (in German)

Harada, Y., Maruyama, Y., Maeda, A., Chino, E., et al. (2000). "Evaluation of High Temperature Tensile and Creep Properties of Light Water Reactor Coolant Piping Materials for Severe Accident Analyses", *Journal of Nuclear Science and Technology*, Vol. 37(6), pp. 518-529.

Harada, Y., Maruyama, Y., Maeda, A., Shibazaki, et al. (2012). "Effect of Microstructure on Failure Behavior of Light Water Reactor Coolant Piping under Severe Accident Conditions", *Journal of Nuclear Science and Technology*, Vol. 36(10), pp. 923-933.

Humphries, L., et al. (2002). *OECD Lower Head Failure Project Final Report*, NEA/CSNI/R(2002)27.

Kasahara, N., Nakamura, I., Machida, H., Nakamura, H. (2015). "Identification of failure modes under design extension conditions", *ASME PVP Conference*, PVP2015-45381, Boston, MA, USA.

Kato, S., Hasebe, S., Yoshida, E. (2008). *Expansion of high temperature creep test data for failure evaluation of BWR lower head*, JAERI, 2007-091.

Krompholz, K., Kalkhof, D. (2002). "Size effect studies of the creep behaviour of a pressure vessel steel at temperatures from 700 to 900 °C". *Journal of Nuclear Materials*, Vol. 305, pp. 112-123.

Larson, F.R., Miller, J. (1952). "A Time-Temperature Relationship for Rupture and Creep Stresses", *Transactions of ASME*, 1952

Maruyama, K. (2008). *Creep Resistant Steels*, Chapter 12: Fracture mechanism map and fundamental aspects of creep fracture, Woodhead Publishing.

Obst, V., Maile, K. (1989). *Versuche zur Schaffung einer Datenstruktur für die inelastische Berechnung von Kriechvorgängen in thermisch belasteten Komponenten*, MPA Stuttgart, Abschlussbericht 1500785. (in German)

Onizawa, T., Wakai, T. (2019). "Development of extremely high temperature material property equations and physical property values on austenitic stain-less steel", SMiRT-25, Charlotte, NC, USA.

Pilch, M., Rashid, Y., Ludwigsen, J., Chu, T. (1998). "Creep Failure of a Reactor Pressure Vessel Lower Head Under Severe Accident Conditions", ASME/JSME joint PVP, San Diego, CA, USA

Rempe, J., Chavez, S., Thinnes, G., Allison, C., et al. (1993). *Light Water Reactor Lower Head Failure Analysis*, INL, NUREG/CR-5642.

Rice, J. R., Tracey, D. M. (1969). "On the ductile enlargement of voids in triaxial stress fields", *Journal of Physics and Mechanics of Solids*, Vol. 17, pp. 201-217.

Ringel, M., Stelling, O. (2005). *Beschreibung des Kurzzeitstandverhaltens bei auslegungsüberschreitenden Temperaturen bis 1200 °C auf der Basis von Schädigungsmechanismen*, MPA-Stuttgart, Abschlussbericht 1501257. (in German)

Rösler, J., Harders, H., Bäker, M. (2012). *Mechanisches Verhalten der Werkstoffe*. 4th edition, Springer Vieweg.

Sainte Catherine, C. (1998). *Tensile and Creep Tests Material Characterisation of Pressure Vessel Steel (16MND5) at High Temperatures (20 up to 1300°C)*, CEA, SEMT/LISN/RT/98-009/A.

Schemmel, J., Schellenberg, D. (1999). *Ermittlung und Modellierung des Werkstoffverhaltens von Reaktorbaustählen unter mehrachsialer Beanspruchung für den auslegungsüberschreitenden Temperaturbereich von 400 °C bis 1000 °C*, MPA Stuttgart, Abschlussbericht 1501010. (in German)

Shimomura, K., Onizawa, T., Kato, S., Ando, M., Wakai, T. (2017). "The Formulation of Material Characteristics of Austenitic Stainless Steels at Extremely High Temperature", ASME PVP Conference, PVP2017-65666. Waikoloa, Hawaii, USA.

Swift, H. W. (1952). "Plastic Instability Under Plane Stress", *Journal of the Mechanics and Physics of Solids*, Vol. 1, pp. 1-18.

Thinnes, G., Korth, G., Chavez, S., Walker, T. (1994). "High-temperature creep and tensile data for pressure vessel steels SA533B1 and SA508-CL2", *Nuclear Engineering and Design*, Vol. 148, pp. 343-350.

Weber, G., Schick, M. (1999). *Heißzug- und Schweißsimulationsversuche an austenitischen Stählen für den Einsatz in Leichtwasserreaktoren*, MPA Stuttgart, Technischer Bericht SR 2235. (in German)

Webster, G., Ainsworth, R. (1994). *High Temperature Component Life Assessment*, Chapman & Hall.

Wilshire, B., Battenbough, A.J. (2007). Creep and creep fracture of polycrystalline copper. Material Science and Engineering A, Vol. 443, pp. 156-166

Whittaker, M.T., Harrison, W. (2014). "Evolution of Wilshire equations for creep life prediction", *Materials at High Temperatures*, Vol. 31, pp. 233-238.

Willschütz, H.-G. (2005). *Thermomechanische Modellierung eines Reaktordruckbehälters in der Spätphase eines Kernschmelzunfalls*, Dissertation, Technische Universität Dresden. (in German)

Willschütz, H.-G., Altstadt, E. (2002). *Generation of a High Temperature Material Data Base and its Application to Creep Tests with French or German RPV-steel*. FZR, FZR-353

Yamaguchi, Y. e. (2020). "Expansion of high temperature creep test data for failure evaluation of BWR lower head in severe accident", *Mechanical Engineering Journal*, Vol. 7(3)